

Observation of three-dimensional bulk Fermi surfaces for a strongly correlated material by soft x-ray h \hbar -dependent (700–860 eV) ARPES

M. Yano,¹ A. Sekiyama,¹ H. Fujiwara,¹ T. Saita,¹ S. Imada,¹ T. Muro,² Y. Onuki,³ and S. Suga¹

¹Division of Materials Physics, Graduate School of Engineering Science,
Osaka University, Toyonaka, Osaka 560-8531, Japan

²Japan Synchrotron Radiation Research Institute, Spring-8, Mikazuki, Hyogo 679-5198, Japan

³Department of Physics, Graduate School of Science,
Osaka University, Toyonaka, Osaka 560-0043, Japan

(Dated: November 18, 2021)

Three-dimensional Fermi surfaces at a high temperature have been clarified for a strongly correlated Ce compound, ferromagnet CeRu₂G_{e₂} in the paramagnetic phase, by virtue of a soft x-ray h \hbar -dependent (700–860 eV) ARPES. Although the observed Fermi surfaces as well as quasiparticle dispersions are partly explained by a band-structure calculation based on a localized 4f model, qualitative discrepancy in experiments, between our ARPES in the paramagnetic phase and de Haas-van Alphen measurement in the ferromagnetic phase, is revealed. This suggests a fundamental change in the 4f contribution to the Fermi surfaces across the magnetic phase transition widely seen for Ce compounds.

PACS numbers: 71.18.+y, 71.27.+a, 79.60.-i

Many macroscopic properties of solids such as resistivity, specific heat and susceptibility depend strongly on momentum distribution of electrons on the chemical potential, namely, shapes and characters of the Fermi surfaces. Therefore, detection of the Fermi surfaces is important to clarify the electronic properties of solids. The quantum oscillation measurement using de Haas-van Alphen (dHvA) effect is known as a powerful technique to observe the cross-sections of the Fermi surfaces [1]. The dHvA measurement has so far been applied also for many strongly correlated rare-earth materials [2, 3, 4]. Since the successful consistency between the experimentally observed Fermi surfaces and the band-structure calculation assuming itinerant 4f electrons for CeSn₃ [5, 6], the dHvA measurement has been recognized as a convincing tool to qualitatively judge whether the 4f electrons are "itinerant" or "localized" for the ground state of strongly correlated Ce compounds. However, the Fermi surfaces at high temperature above several tens K, at which the electronic structures are often deviated from the ground state due to magnetic phase transitions and/or the Kondo effect, have not been experimentally clarified for many Ce compounds because a low temperature is required for the dHvA measurement. The low-h \hbar -angle-resolved photoemission spectroscopy (ARPES) is also useful to reveal the characters of the two-dimensional and/or surface Fermi surfaces as seen in the results for high-T_C cuprates [7]. As for the rare-earth compounds, ARPES measurements for XRu₂S₂ (X = La, Ce, Th, U) have been performed by using h \hbar in a 14–230 eV range [8]. Recently high-energy (h \hbar > 500 eV) photoemission is found to be very effective in probing bulk states [9, 10, 11, 12]. In this letter, we demonstrate the power of soft x-ray h \hbar -dependent ARPES for clarifying the bulk three-dimensional Fermi surface topology of a strongly correlated rare-earth compound, whose 4f electronic states are mutually different between the bulk and surface [10].

We have performed the ARPES measurements for CeRu₂G_{e₂} which has one 4f electron per unit cell then we have compared with the band calculation for 4f electron localized model. LaRu₂G_{e₂}. CeRu₂G_{e₂} is a requisite material to understand the electronic states of Ce heavy fermion systems because the rather localized 4f electrons become itinerant under high pressures [13]. CeRu₂G_{e₂} is a ferromagnet with T_C = 8 K [14, 15] and the 4f electrons of CeRu₂G_{e₂} are thought to be localized because RKKY interaction is dominant compared with the Kondo effect at low temperatures with the electronic specific heat coefficient of about 20 mJ/m³molK⁻² [14] and the Kondo temperature T_K < 1 K [16, 17]. CeRu₂G_{e₂} crystallizes in a tetragonal ThCr₂S₂-type structure with a = 4.268 Å and c = 10.07 Å at 18 K [14] and its Brillouin zone is shown in Fig. 1 (a). On the other hand, isostructural CeRu₂S₂ has itinerant 4f electrons with its low-temperature electronic specific heat coefficient of about 350 mJ/m³molK⁻² [18] and T_K = 20 K [17]. These properties are consistent with the bulk sensitive 3d–4f resonant photoemission results [10]. The larger lattice constant of CeRu₂G_{e₂} than that of CeRu₂S₂ makes such different 4f electron properties.

CeRu₂G_{e₂} single crystal was grown by the Czochralski pulling method. The high energy ARPES measurements have been performed from h \hbar = 700 to 860 eV with an energy step of 5 eV at BL25SU in Spring-8 [19]. The light incidence angle was 45 degrees with respect to the sample surface normal. The base pressure was about 3 × 10⁻⁸ Pa. We have performed the measurements at 20 K, where the sample was in the paramagnetic phase. The clean surface was obtained by cleaving in situ providing a (001) plane. A GAMMADATA-SCIENTA SES200 analyzer was used covering more than a whole Brillouin zone along the direction of the slit. The energy resolution was set to 200 meV for Fermi surface mapping. The cleanliness was confirmed by the absence of the O 1s and C 1s photoemission signals. First, we have performed k_z = k_{xy}

mapping at several k_z and angles. After determining the k_z corresponding to the high symmetry points along the [001] direction, we have performed detailed angle-dependent ARPES for k_x - k_y mapping. Then we have performed k_z dependent ARPES for k_z - k_{xy} mapping through the high symmetry points in the k_{xy} Brillouin zone.

In order to experimentally determine the exact value of $|k_z|$ we have taken the incident photon momentum into account. If x-ray was incident onto a sample at 45 degrees with respect to the surface normal, for example, this incident photon has the momentum parallel (k_{\parallel}) and perpendicular (k_{\perp}) to the surface, which are $2k_{\parallel} = \frac{P}{\hbar}$ (\AA^{-1}) = $2\hbar$ (eV) = $12398 \frac{\text{\AA}^{-1}}{\text{eV}}$. In the case of $\hbar = 700$ eV, the photon momentum values of both $|k_{\parallel}|$ and $|k_{\perp}|$ are about 0.25\AA^{-1} . Because the value $|k_z|$ of the 1st Brillouin zone of CeRu_2Ge_2 ($2\pi/c = 0.62 \text{\AA}^{-1}$) is comparable to the value of the photon momentum, both k_{\parallel} and k_{\perp} cannot be negligible.

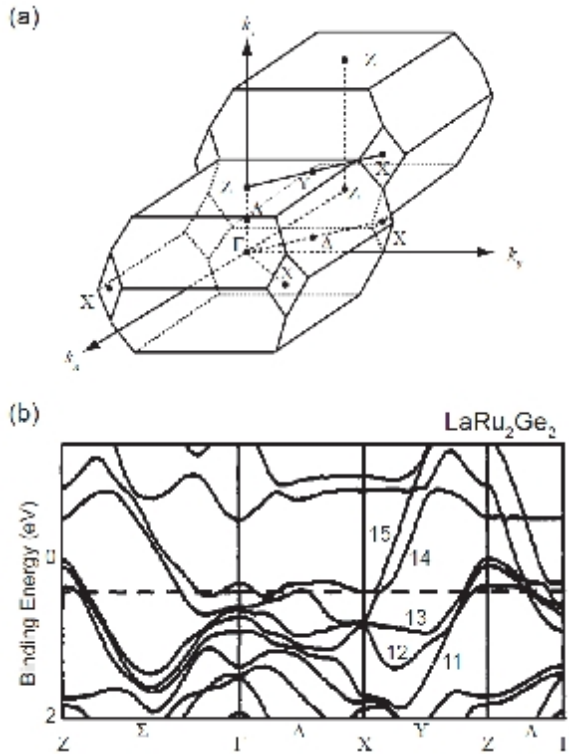


FIG. 1: (a) The Brillouin zone of the body-centered tetragonal crystal CeRu_2Ge_2 with $|a| = |b| = 2c$. (b) The band calculation with APW method for LaRu_2Ge_2 [20]. The Fermi surfaces are formed by 5 bands from 11 to 15.

The observed ARPES data have been compared with the band calculation of paramagnetic LaRu_2Ge_2 performed by H. Yamagami and A. Hasegawa [20] with using a symmetrized relativistic augmented-plane wave (APW) method [21]. According to their calculation, five bands (11 - 15) cut the Fermi level (E_F) (Fig. 1(b)) forming five Fermi surfaces which are composed of the La 4d and

Ru 4d states. Five Fermi surfaces are likewise derived for the itinerant 4f electron system CeRu_2Si_2 [22]. Between the localized LaRu_2Ge_2 and itinerant CeRu_2Si_2 , the shapes of Fermi surfaces derived from the bands 11 to 14 are not much different but the shape of the band 15 is mutually different. Among the calculated bands of LaRu_2Ge_2 , the lower four bands from 11 to 14 form the hole-like Fermi surfaces which are centered at the Z point in the Brillouin zone, and the highest band 15 forms the electron-like Fermi sheet.

Figure 2(a) shows the energy distribution curves (EDCs) along the in-plane X - Z - X direction for CeRu_2Ge_2 . The positions of the wave number where each band cuts E_F is also estimated by the momentum distribution curves (MDCs). Five bands corresponding to the bands 11 to 15 predicted by the band calculation for LaRu_2Ge_2 are clearly seen. There is a clear peak near E_F at the Z point in Fig. 2(a). The presence of this peak is in a strong contrast to the result of the band-structure calculation for LaRu_2Ge_2 , which predicts no quasiparticle peak near E_F at the Z point in Fig. 1(b). It is thus revealed that the band 11 is located on the occupied side and does not form the Fermi surface. Although the band 15 does not cut E_F at the X point in the calculation for LaRu_2Ge_2 , our experimental results show that the band 15 exists on the occupied side at the X point. Figure 2(b) shows EDCs along the in-plane Z - Z direction. The comparison between Fig. 1(b) and Fig. 2 has shown the similarity of the observed bands 15 and 14 in CeRu_2Ge_2 with the result of the band calculation of LaRu_2Ge_2 .

Figure 3 displays Fermi surfaces' topology at $k_z = 2\pi/c$ by integrating the intensity around E_F of EDCs. The X - Z - X line corresponds to Fig. 2(a). The intensities around the Z point are due to the bands 11-13. We have clearly observed the small Fermi surface contours around the Z point derived from both bands 12 and 13 and the large Fermi surface contour derived from the band 14 as judged from Fig. 2(a). Furthermore, we recognize a small Fermi surface contour centered at the X point. The possible origin of this small Fermi surface is the band 15, whereas its E_F crossing is not predicted by the calculation for LaRu_2Ge_2 .

Figure 4 demonstrates Fermi surfaces' topology at $k_z = 0$. The Z - Z line corresponds to Fig. 2(b). The very large Fermi surface derived from the band 14 is clearly seen around the Z points. Furthermore a part of the Fermi surface derived from the band 15, whose shape looks like a doughnut centered at the Γ point according to the calculation for LaRu_2Ge_2 , can be traced.

Meanwhile, Fig. 5 shows the Fermi surface slice at $k_z = k_{xy}$ plane measured with an energy step of 5 eV. In this figure are recognized the Fermi surfaces 12 and 13 centered at the Z point, which are prolonged along the k_z direction. The very large Fermi surface 14 compressed vertically can be also experimentally traced. Along the horizontal X - X direction, the band 15 cuts E_F near the Γ and X points. The Fermi surface of the band 15 is only partly observed near the Γ point because of

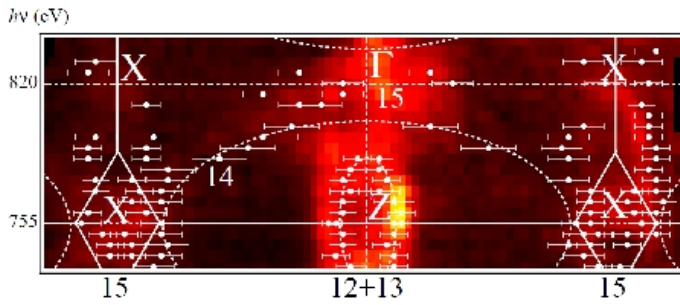


FIG. 5: (color online) Fermi surface slice in k_z (ordinate) - k_{xy} (abscissa) plane. Photon energies were changed from 735 eV to 840 eV. $h\nu = 820$ eV and 755 eV correspond to the Γ point and the Z points, respectively, along the Γ -Z direction corresponding to the right most zone in Fig.1 (b). The upper horizontal X - X axis corresponds to the second zone from the left in Fig. 1 (b). Photoemission intensity map was obtained by integrating the PES intensity from +0.1 eV to -0.1 eV.

contrast to the dHvA results in the ferromagnetic phase. Although the Fermi surface of CeRu_2Ge_2 in the ferromagnetic phase is similar to that of LaRu_2Ge_2 , the difference of our ARPES results from them are consistently understood if E_F of CeRu_2Ge_2 in the paramagnetic phase is energetically higher than that of the calculation for LaRu_2Ge_2 . E_F shift of CeRu_2Ge_2 in the paramagnetic phase from LaRu_2Ge_2 or CeRu_2Ge_2 in the ferromagnetic phase is thought to be due to the increased number of the electrons contributing to the near E_F bands in CeRu_2Ge_2 , where the weak but nonnegligible hybridization of the Ce 4f electron should be additionally taken into account in the paramagnetic phase. The difference of the electric resistivity between CeRu_2Ge_2 and LaRu_2Ge_2

is suddenly diminished below T_C of CeRu_2Ge_2 [14], indicating the reduction of electron scattering by the ferromagnetic ordering. This suggests that the contribution of the 4f electrons to the Fermi surfaces due to the hybridization is reduced in the ferromagnetic phase. Then the number of the electrons contributing to the Fermi surfaces decreases below T_C . Accordingly, the band 11 crosses E_F near the Z point and the band 15 might form discontinuous Fermi surfaces along the X - X (k_z) direction as predicted by the band-structure calculation.

We have performed three-dimensional bulk-sensitive ARPES measurements for paramagnetic CeRu_2Ge_2 by using soft x-rays. Although the Fermi surfaces obtained for the bands 12, 13 and 14 are in good agreement with the result of the band calculation for paramagnetic LaRu_2Ge_2 , the predicted band 11 is found to be not contributing to the Fermi surface in paramagnetic CeRu_2Ge_2 . The band 15 is confirmed to have the doughnut-like shape around the Γ point whereas a rod-like continuous Fermi surface along the X - X axis is observed in a strong contrast to the band calculation. The slight hybridization in the paramagnetic phase and the magnetic ordering below T_C are thought to be essential to understand the behaviors of three-dimensional electronic structures of CeRu_2Ge_2 .

We are grateful to H. Yamagami for fruitful discussions. We thank T. Miyachi and H. Higashimichi for their help in the experiments. The present work was performed at Spring-8 under the proposal (2004A 6009-NS- ν p, 2004B 0400-NS- ν p) supported by the Grant-in-Aid for Creative Scientific Research (15GS0213) of MEXT Japan and 21st Century COE program (G18) of Japan Society for Promotion of Science.

-
- [1] N. W. Ashcroft, and N. D. Mermin, 1976, Solid State Physics (Saunders College, Philadelphia).
- [2] H. Yamagami and A. Hasegawa, J. Phys. Soc. Jpn. 60, 1011 (1991).
- [3] P. H. P. Reinders, M. Springford, P. T. Coleridge, R. Boulet, and D. Ravot, Phys. Rev. Lett. 57, 1631 (1986).
- [4] G. Zwicknagl, Adv. Phys. 41, 203 (1992).
- [5] W. R. Johanson, G. W. Crabtree, A. S. Edelstein and O. D. Mcasters, Phys. Rev. Lett. 46, 504 (1981).
- [6] A. Hasegawa et al., J. Phys. Soc. Jpn. 59, 2457 (1990).
- [7] A. Damascelli, Z. Hussain, and Z.-X. Shen, Rev. Mod. Phys. 75, 473 (2003).
- [8] J. D. Denlinger et al., J. Electron Spectrosc. Relat. Phenom. 117, 347 (2001).
- [9] A. Sekiyama et al., Nature (London) 403, 396 (2000).
- [10] A. Sekiyama et al., J. Phys. Soc. Jpn. 69, 2771 (2000).
- [11] A. Sekiyama et al., Phys. Rev. B 70, 060506(R) (2004).
- [12] S. Suga et al., Phys. Rev. B 70, 155106 (2004).
- [13] H. Wilhelm and D. Jaccard, Phys. Rev. B 69, 214408 (2004).
- [14] M. J. Besnus et al., Physica B 171, 350 (1991).
- [15] A. Bohm et al., J. Magn. Magn. Mater. 76-77, 150 (1988).
- [16] A. Loidl et al., Phys. Rev. B 46, 9341 (1992).
- [17] A. Loidl, G. Knopp, H. Spille, F. Steglich, A. P. Murani, Physica B 156, 794 (1989).
- [18] G. G. Lonzarich, J. Magn. Magn. Mater. 76-77, 1 (1988).
- [19] Y. Saitoh et al., J. Synchrotron Rad. 5, 542 (1998).
- [20] H. Yamagami and A. Hasegawa, J. Phys. Soc. Jpn. 63, 2290 (1994).
- [21] H. Yamagami and A. Hasegawa, J. Phys. Soc. Jpn. 59, 2426 (1990).
- [22] H. Yamagami and A. Hasegawa, J. Phys. Soc. Jpn. 62, 592 (1993).
- [23] C. A. King and G. G. Lonzarich, Physica B 171, 161-165 (1991).
- [24] H. Ikezawa et al., Physica B 237, 210 (1997).